Hydrogen-Bonding in Cardo Copoly(aryl ether ketone)s and Its Effects on the Gas Permeation Behavior

Zhonggang Wang,*,† Tianlu Chen,‡ and Jiping Xu‡

Department of Polymer Science and Materials, School of Chemical Engineering, Dalian University of Technology, Zhongshan Road 158, Dalian, 116012, P. R. China, and Changchun Institute of Applied Chemistry, Chinese Academy of Sciences, Changchun, 130022, P. R. China

Received February 16, 2007; Revised Manuscript Received March 7, 2007

ABSTRACT: A series of hydrogen-bonded cardo poly(aryl ether ketone) copolymers were prepared by polymerization from a mixture of phenolphthalein (PPH) and 3,3′-bis(4-hydroxyphenyl)isobenzopyrrolidone (HPP) with equivalent molar bis(4-nitrophenyl) ketone. The gas permeabilities of H_2, O_2, and N_2 through copolymer membranes were examined over a temperature range of 30−100 °C. In comparison with bisphenol A polysulfone (PSF), all the homo- and copolymers exhibited similar H_2 permeability coefficients, but H_2/N_2 selectivity coefficients were more than twice as high as that of PSF. Of interest was the observation that, different from previous other copolymers, the gas permeability in this study exhibited a sigmoid dependency on comonomer composition, and the variation amplitude of gas permeability coefficients between wave trough (40 mol % HPP) and wave crest (60 mol % HPP) was reduced with increased temperature. This peculiar phenomenon was interpreted according to polymeric structural factors, including free volume, interchain distance, glass transition, secondary transition, and the effect of temperature on interchain hydrogen bonds.

Introduction

Over the past two decades, many new polymeric membrane materials for gas separation emerged, including poly(aryl ether)s,[1−4] polyarylates,[5,6] poly(1-trimethylsilyl-1-propyne)s,[7,8] polyimides,[9−11] polyamides,[12] polynorbornenes,[13] and poly(2,6-dimethyl-1,4-phenylene oxide)s,[14−16] etc. However, in spite of the great collection of available gas permeability data, the understanding of structure−property relationship is still insufficient. The previously published studies revealed that gas permeability through polymer membrane could be affected by a variety of factors, such as chemical structure of main/side chain, length and size of side chain, stereoconfiguration, conformation, polarity, cohesive energy density, intra- and interchain interaction, crystallinity, packing density, and glass transition and secondary transition of polymer chains.[17−20] In order to synthesize well-defined polymers possessing predetermined high gas permeability coefficient (P) and selectivity coefficient (α), more accurate knowledge of the specific function of a single physical parameter on the gas permeation behavior is essential for both the industrial and academic field. For the purpose of structure−property relationship research, polymer structures must be carefully designed, in which it is desirable that only one or two polymer structural parameters are systematically varied while maintaining other physical factors constant to a great extent.

In comparison with the large amount of reports on gas permeation behavior of homopolymers at ambient temperature, only relatively limited information is available on the gas transport of copolymers,[21−23] in particular the high-temperature gas permeation aspect. As a matter of fact, the copolymerization modification can be a simple and convenient way to achieve a useful combination of the advantages of two polymers into a new polymer. Moreover, by means of precisely adjusting the molar ratio of two components in copolymer, the effect of certain specific structural factor on gas permeability may be quantitatively investigated. On the other hand, from the energy saving point of view, in some cases, the membrane separation applications are operated at elevated temperature. The ideal polymeric materials for membranes used for gas separation should possess not only high gas permeability and high selectivity but also excellent mechanical toughness and thermal stability. In this regard, the study on temperature dependency of gas transport properties is of great importance.

Phenolphthalein-based cardo poly(aryl ether ketone) (PEK-C) has attracted much attention because of its properties such as thermooxidative stability, high glass transition temperature, good membrane-formation property, and gas permeability and selectivity. With an effort to further improve its gas transport properties, in our previous papers, a series of chemical modifications on PEK-C had been carried out. For example, introducing different alkyl substituents onto phenyl ring to enhance the free volume of polymer, attaching pendent amide and carboxyl groups onto the PEK-C backbone to yield interchain hydrogen bonds, or manipulating the length/diameter ratio of polymer repeat unit to change the regularity of polymer chain. The results demonstrated that the subtle variation in chemical structure could bring about significant effects on the polymeric segmental mobility, chain packing density, interchain interaction, and gas transport properties.[19,24−27] PEK-H is another high-T_g (263 °C) cardo poly(aryl ether ketone) synthesized in our laboratory, which has very similar chemical structure to PEK-C with an only difference in that PEK-H has a pendent lactam group instead of a lactone group in PEK-C (Scheme 1), while the pendent lactam group can lead to PEK-H strong interchain hydrogen bonds.

In this study, the PEK-C/PEK-H random copolymers with comonomer composition from 0 to 100 mol % were synthesized using the same polycondensation condition. The gas transport properties of various gases through polymer membranes were measured over a temperature range from 30 to 100 °C. The systematic variations in interchain hydrogen-bonding degree by

* To whom all correspondence should be addressed. E-mail: zgwang@dlut.edu.cn.
† Dalian University of Technology.
‡ Chinese Academy of Sciences.

10.1021/ma070426z CCC: $37.00
Published on Web 04/03/2007

Scheme 1. Chemical Structures of PEK-C and PEK-H Homopolymers

PEK-C

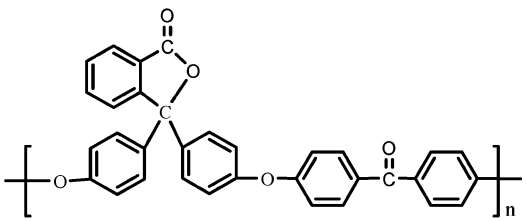

PEK-H

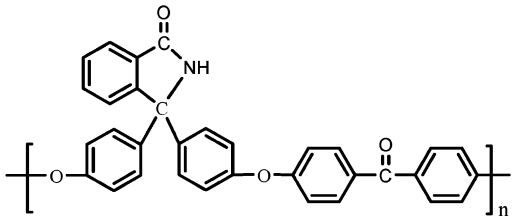

changing the number and distribution of lactam groups in the polymer backbone were expected to yield interesting effects on conformation, molecular motion, and aggregative structure of polymer chains and, hence, should significantly influence the gas permeation behavior through polymer membranes. The study methods include temperature-dependent FTIR spectroscopy, X-ray diffraction, density measurement, differential scanning calorimetry, dynamic mechanical thermal analysis, and gas permeability measurement.

Experimental Section

Materials. Phenolphthalein (PPH) was purchased from Beijing Chemical Works and purified by recrystallization from 50:50 (v/v) mixed solvent of ethanol and water (mp 262−263 °C); bis(4-nitrophenyl) ketone (DNDPK) was prepared in our laboratory (mp 189−190 °C); bis(4-chlorophenyl) sulfone (DCDPS) was purchased from the Beijing Chemical Plant and purified by recrystallization from ethanol; dimethyl sulfoxide (DMSO) and *N*,*N*-dimethylformamide (DMF) were purified by vacuum distillation just before use; anhydrous potassium carbonate was finely powdered prior to use; 3,3′-bis(4-hydroxyphenyl)isobenzopyrrolidone (HPP) was prepared in our laboratory according to ref 28.

All the poly(aryl ether ketone) homopolymers and copolymers were prepared via nucleophilic polycondensation in DMSO using K_2CO_3 as catalyst. A typical procedure for PEK-C/PEK-H copolymer with 50 mol % of HPP content was described as follows: to a solution of 4.1462 g (0.03 mol) of anhydrous K_2CO_3, 12 mL of toluene, and 11.8 mL of DMSO, 4.8052 g (0.015 mol) of PPH and 4.7749 g (0.015 mol) of HPP were added. A slow stream of nitrogen was maintained throughout the whole reaction. The temperature was raised to 140 °C to remove water formed by azeotropic distillation with toluene for about 2 h, and then the toluene was distilled out and temperature was raised gradually to 175 °C, allowed to react at this temperature for an additional 2 h, and finally a viscous solution was obtained. After cooling, it was diluted with DMF and settled overnight. The supernatant liquid was coagulated in mixed precipitant of ethanol and water to separate the white polymer. The polymer was washed successively with boiling water to remove the inorganic salt and dried in air at 100 °C for 12 h.

As a comparison, the bisphenol A polysulfone (PSF) was prepared from bisphenol A with bis(4-chlorophenyl) sulfone in the same condition above.

Dense Film Preparation. The polymer samples were dissolved in DMF to form a solution of 10 wt %, which was cast onto a clean glass plate at 60 °C in an oven for 8 h. After most solvent evaporated, the film was stripped from glass plate and transferred to vacuum oven and dried further at 200 °C and 10 mmHg for 48 h. Films thick were 45−50 μm.

Measurements. Reduced viscosities were measured using a Ubbelohde viscometer at a concentration of 0.5% (w/v) in DMF at 25 ± 0.01 °C.

The temperature-dependent FTIR spectra were recorded on a Digilab FTS-20E FTIR spectrometer equipped with a heatable copper accessory. Film samples of 5 μm thickness were vacuum-dried at 180 °C for at least 24 h before measurement. The corresponding temperature for the desired measurement was controlled manually. All spectra were baseline corrected.

Glass transition temperatures (T_gs) were determined on Perkin-Elmer DSC-7 over a temperature interval of 100−400 °C at a heating rate of 20 °C/min. T_gs were read at the middle of the change in the heating capacity. A simple method to estimate the T_g values of random copolymers by the Fox equation is as follows:[29]

$$\frac{1}{T_g} = \frac{w_1}{T_{g_1}} + \frac{w_2}{T_{g_2}} \tag{1}$$

where w_1 and w_2 are the weight fractions and T_{g_1} and T_{g_2} are the glass transition temperatures of two homopolymers.

Wide-angle X-ray diffraction (WAXD) measurements were performed at room temperature (about 25 °C) on a D/Max-B X-ray diffractometer, using Cu KR radiation at a wavelength of 1.54 Å (40 kV, 15 mA). The scanning rate was 2°/min over a range of 2θ = 5°−40°.

Dynamic mechanical thermal analysis (DMTA) was performed on film samples using RHEOVIBRON-DDV-II-E_A (Japan), at a frequency of 3 Hz and a heating rate of 4 °C/min from −150 to 350 °C. The preparation and after-treatment of the film samples are completely same as that used for the gas permeability measurement.

Polymer densities were determined in film sample in a density gradient column containing aqueous solution of calcium nitrate at 30 ± 0.1 °C.

Free volume (V_F) of each of the polymers is given by the following equation:

$$V_F = V_T - V_0 \tag{2}$$

where V_T is specific volume, which can be calculated from the polymer density determined; V_0 is the polymer occupied volume in 0 K and was obtained according to the group contribution method of Sugden.[30]

Pure gas permeability coefficients over the temperature interval of 30−100 °C for H_2, O_2, and N_2 were measured by a vacuum manometric method with an upstream pressure of 5 atm. The permeation cell temperature was controlled within ±0.2 °C and was measured by a calibrated Cu−constantan thermocouple inserted just above the membrane in the permeation cell. All the gases used here were at least 99.99% in purity. The permeability coefficient (P) was obtained from the slope of pressure−time plots after a steady state has been reached. The ideal separation factor ($\alpha_{A/B}$) of gas A over another gas B is given by the equation

$$\alpha_{A/B} = P_A/P_B = (D_A/D_B)(S_A/S_B) \tag{3}$$

where P_A and P_B are the permeability coefficients for gases A and B, respectively.

Results and Discussion

Physical Properties. PEK-C and PEK-H homopolymers and their copolymers were synthesized via solution nucleophilic polycondensation at the same reaction condition. The copolymers prepared here were named as PEK-AB, in which A and B was described as the molar percentage of PEK-C and PEK-H components, respectively. The reduced viscosities for all the polymer samples were controlled to a narrow range of 0.52−0.61 dL/g so that an effective physical properties comparison could be made only based on the molecule structure. The

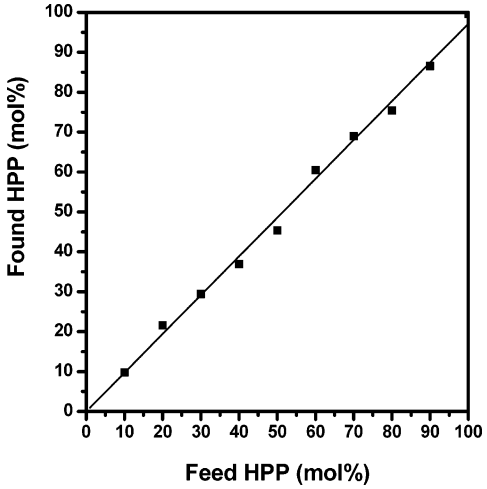

Figure 1. Comonomer composition in PEK-C/PEK-H copolymers measured by IR spectroscopy.

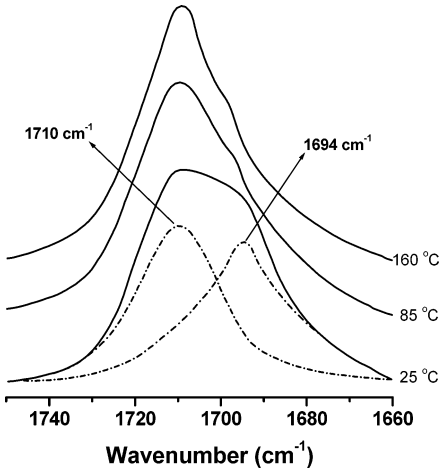

Figure 2. Temperature-dependent FTIR spectra of PEK-H.

copolymers showed characteristic IR absorptions of Ar−CO−Ar at 1645 cm^{-1}, Ar−O−Ar at 1245 cm^{-1}, lactone carbonyl at 1772 cm^{-1}, and lactam carbonyl at 1701 cm^{-1}. The comonomer compositions were quantitatively measured using the integrated peak area of two characteristic absorptions of 1772 and 1701 cm^{-1}, which were well consistent with the feed ratios (see Figure 1).

The occurrence of hydrogen bonding in PEK-H was confirmed by temperature-dependent FTIR spectroscopy. Since the hydrogen bond between N−H and carbonyl oxygen of lactam group weakened the force constant of C═O double bond, the carbonyl absorption was found to shift toward a lower wavenumber. As shown in Figure 2, the broad carbonyl absorption in the vicinity of 1701 cm^{-1} at ambient temperature could, in fact, be resolved into two peaks. The peak at 1710 cm^{-1} was related to free C═O stretching vibration and the peak at 1694 cm^{-1} to hydrogen-bonded C═O stretching of the lactam group. Upon heating the sample from 25 to 160 °C, the 1694 cm^{-1} absorption shifted toward high frequency, and a sudden drop in intensity took place. The drop in intensity was due to the enhanced polymeric segmental mobility at high temperature, which broke some of the associated hydrogen bonds and led to the decreased number of hydrogen bonds.

The DSC measurements gave the glass transition temperatures of PEK-C and PEK-H of 218 and 263 °C, respectively. As a measure of the rigidity of the polymer chain, the glass transition temperature of PEK-H is 45 °C higher than that of PEK-C,

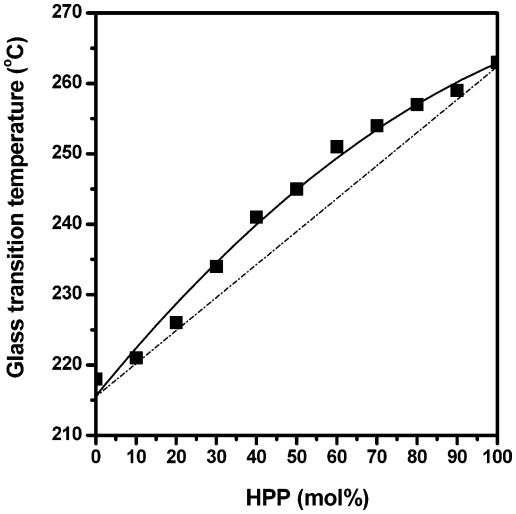

Figure 3. Glass transition temperatures as a function of comonomer composition.

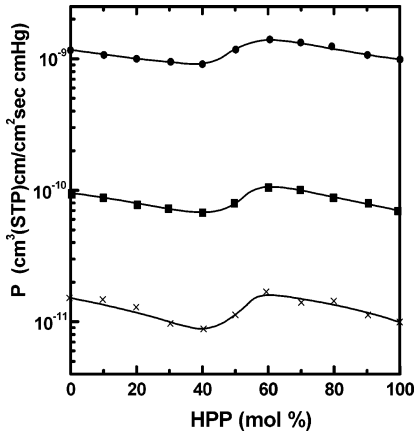

Figure 4. Relationship between permeability coefficients and HPP content: (●) H_2; (■) O_2; (×) N_2.

indicating that the interchain hydrogen bonds restricted the segmental motion ability. All the DSC curves for copolymers show a single T_g transition, which increased steadily with the HPP content. However, as shown in Figure 3, the experimental T_g values obtained from DSC measurements (solid line) were higher than those calculated from Fox equation (dashed line), exhibiting the positive deviation from the linear additive rule. Similar phenomena have also been observed for other random copolymer system, such as 6FDA-DDS/6FDA-6FAP copolyimides[31] as well as miscible blends of polymers, such as the blends of poly(amic acids) with poly[2,2′-(*m*-phenylene)-5,5′-bibenzimidazole],[32] poly(*p*-vinylphenol) with poly(2-vinylpyridine)-*block*-poly(ethylene oxide),[33] PHFA with poly(butyl methacrylate), and poly(styrene-*co*-vinylphenylbis(trifluoromethyl)carbinol) with polycarbonate systems,[34] etc. The main reason for the upper convex form of the T_g diagram was explained as strong hydrogen-bonding interactions.

Gas Transport Properties. Gas permeability and selectivity coefficients of three gases through the homopolymer and copolymer membranes are summarized in Table 1. The gas transport properties of PSF membrane were measured with the same parameters and also listed as a comparison. All the polymers had similar H_2 permeability coefficient, but H_2/N_2 selectivity coefficients were more than twice as high as that of PSF, exhibiting potential in H_2/N_2 separation application. A number of literatures have revealed that separation of smaller

Table 1. Gas Transport Properties of Copolymers at 30 °C

	P (barrer)			α	
sample	H_2	O_2	N_2	H_2/N_2	O_2/N_2
PEK-C	11.7	0.952	0.154	76.0	6.18
PEK-1090	10.5	0.867	0.140	75.0	6.19
PEK-2080	10.4	0.786	0.125	83.2	6.29
PEK-3070	9.74	0.734	0.0938	103.8	7.82
PEK-4060	8.71	0.630	0.0828	105.2	7.61
PEK-5050	9.95	0.731	0.103	96.6	7.10
PEK-6040	13.8	1.11	0.168	82.1	6.61
PEK-7030	11.5	0.904	0.128	89.8	7.06
PEK-8020	11.4	0.861	0.140	81.4	6.15
PEK-9010	10.4	0.748	0.106	98.1	7.06
PEK-H	9.91	0.663	0.0935	106.0	7.09
PSF	10.4	1.24	0.209	49.8	5.93

molecules such as hydrogen from larger molecules such as nitrogen through polymer membrane is mainly affected by the packing density and segmental motion ability of the polymer chain. High permeability is primarily caused by more free volume, while significant increase in gas permselectivity is mainly due to restricted segmental motion.[35−38] The above conclusion could be used to explain the reason for the high gas selectivity coefficients of this series of copolymer membranes. The pendent bulky polar cardo group led to PEK-C and its copolymers very stiff polymer chain structure as demonstrated by its higher glass transition temperature than PSF. Especially, after introducing interchain hydrogen bonds, the segmental motion ability was seriously inhibited, which could be responsible for their high gas selectivity than that of PSF.

H_2, O_2, and N_2 are nonpolar gases, and there are not special interactions between gas and polymer backbone. For each membrane, the permeability of H_2 was the highest, and followed sequentially by O_2 and N_2, which was the same as the order of gas kinetic diameter—σ_{H_2} (2.80 Å) < σ_{O_2} (3.46 Å) < σ_{N_2} (3.64 Å)[39]—but different from the tendency of critical temperature—$T_{c(O_2)}$ (154.6 K) > $T_{c(N_2)}$ (126.2 K) > $T_{c(H_2)}$ (33.2 K).[40] Therefore, the gas permeabilities through copolymer membranes are primarily governed by the kinetic factors, such as kinetic diameter of gas molecule, interchain spacing, packing density, and mobility ability of polymer chains.

Usually, for random copolymers, the relationship between logarithm of permeability and copolymer composition followed the linear additive rule: $\ln P = \phi_A \ln P_A + \phi_B \ln P_B$, where ϕ is the volume fraction, P is the permeability coefficient, and the subscripts A and B refers to the two homopolymers.[22,41,42] Nevertheless, in this study, it was surprisingly found that, for all the gases of H_2, O_2, and N_2, the permeability−composition relationships exhibited sigmoidal curves, appearing the minimum value at 40 mol % HHP and maximum at 60 mol % HPP, which was not in agreement with the additive rule (see Figure 4). To our knowledge, up to now, the sigmoid variation of gas permeability with copolymer composition is rather rare in the literature.

Structure−Property Relationships. The DMTA curves for homo- and copolymers are illustrated in Figure 5. The peak where internal friction (tan δ) went through a maximum was corresponded to glass transition. Other relaxation transitions on the lower temperature side of glass transition were designated as β and γ transitions. Since all the film samples had been treated by annealing, the β and γ transitions should not be caused by nonequilibrium packing defects of polymer chains but were attributed to the small molecule unit rotational movement around the flexible bond in the polymer chain. As shown in Table 2, all the polymer samples had the glass transition temperature above 244 °C. In the temperature range of gas permeability

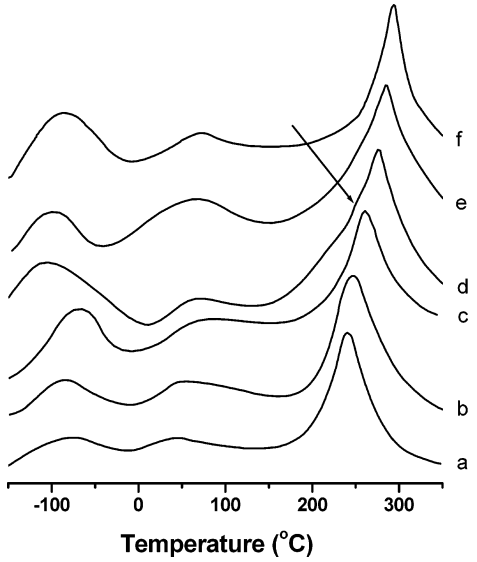

Figure 5. Tan δ as a function of temperature for the four polymers: (a) PEK-C; (b) PEK-2080; (c) PEK-4060; (d) PEK-6040; (e) PEK-8020; (f) PEK-H.

Table 2. Dynamic Mechanical Analysis Data of the Polymers Studied

sample	T_g (°C)	T_β (°C)	T_γ (°C)
PEK-C	244	49	−78
PEK-2040	251	54	−82
PEK-4060	259	78	−59
PEK-6040	264	64	−102
PEK-8020	271	68	−96
PEK-H	289	76	−89

measurements, the membrane samples were in glassy state, and their long-range micro-Brownian motion in molecular chain had been frozen, but secondary transitions were still active. As a consequence, the gas permeability through polymer membrane should be more closely related to the secondary transition other than glass transition. For poly(aryl ether ketone) copolymers, the γ transition involved the motion of pendent lactone or lactam groups occurring at about −80 °C, while the β transition at about 60 °C was associated with the motion of phenyl rings in the polymer backbone around the C−O bond, which had also been observed in related poly(aryl ether)s.[43,44] The interchain hydrogen bonds between lactam groups inhibited the free motion of pendent lactam groups, resulting in PEK-H the higher the β transition temperature in comparison with PEK-C.

Further careful observation on DMTA curves revealed that, for PEK-2080 and PEK-4060, there was only a single sharp glass transition, indicating the homogeneous distribution of HPP in the polymer chain. However, for PEK-6040, the glass transition peak was apparently broadened, and a slight shoulder seemed to appear on the lower temperature side of glass transition. This phenomenon could be attributed to the heterogeneity of the HPP moiety in the polymer chain owing to the different reactive activity between PPH and HPP. Although PPH and HPP have similar chemical structures, their reactive mechanisms are very different. PPH monomer contains the phthalide group and is usually used as an acid−base solution indicator. In the K_2CO_3/DMSO polymerization solution existed the acid−base equilibrium (Scheme 2). During the course of polymerization, PPH was present in the form of quinoid and phenolic isomers, and the equilibrium shifted toward the left with the polymerization proceeding, while HPP bisphenol monomer did not need to go through the isomerization and could directly polymerize with bis(4-nitrophenyl) ketone. Therefore, HPP was more reactive than PPH. The effect of difference in

Table 3. Packing Density Data of PEK-C/PEK-H Copolymers

PPH/HPP (mol % ratio)	ρ (g/cm^3)	$V_{25°C}$ (cm^3/g)	V_0 (cm^3/g)	V_F (cm^3/g)	$1/V_F$ (g/cm^3)
100/0 (PEK-C)	1.249	0.801	0.603	0.128	7.87
90/10	1.250	0.800	0.675	0.125	7.94
80/20	1.245	0.803	0.676	0.127	7.81
70/30	1.255	0.797	0.677	0.120	8.33
60/40	1.261	0.793	0.678	0.115	8.70
50/50	1.253	0.798	0.679	0.119	8.40
40/60	1.229	0.820	0.681	0.139	7.19
30/70	1.238	0.814	0.682	0.132	7.56
20/80	1.241	0.808	0.683	0.125	8.00
10/90	1.247	0.806	0.684	0.122	8.26
0/100 (PEK-H)	1.250	0.802	0.685	0.117	8.57

reactive activity on sequence distribution of copolymer was not obvious at low HPP content, e.g., lower than 40 mol %. Nevertheless, when HPP content was increased to over 50%, in the initial polymerization stage, HPP tended to enrich in the copolymer chain and eventually lead to the heterogeneous distribution of the HPP moiety in copolymer backbone. The local aggregation of intermolecular hydrogen bonds owing to lactam groups in HPP moiety restricted the effective packing of nonassociated polymer segments, while the loose chain packing was favorable for the motion of side group. As a result, PEK-6040 showed the lowest γ transition temperature of −102 °C, while PEK-4060 had the highest γ transition temperature of −59 °C among the copolymers studied (see Table 2).

Intermolecular hydrogen bonds due to the lactam groups yielded a significant effect on the packing density of copolymers, but the change trend of packing density with HPP content was not monotonic. As seen in Table 3, in the initial stage, the free volume steadily decreased with the HPP content until appearing at the minimum value at 40 mol % HPP, then increased suddenly at 50 mol %, reached its maximum at 60 mol %, and decreased again afterward. The possible reasons for this peculiar packing density−composition dependency behavior may be due to the synergistic effect of two opposing factors. Generally speaking, the introduction of strong interchain hydrogen bonds is advantageous for dense chain packing, showing a decreasing free volume with the increase of number of hydrogen bonds, and so it did when the HPP content was below 40%. On the other hand, the introduction of interchain hydrogen bonds seriously inhibits the chain motion ability. For the PEK-C/PEK-H copolymer system, the lactam groups were distributed randomly along the backbone of polymer chain, simultaneously consisting of hydrogen-bond associated and nonassociated polymer segments. The local interchain hydrogen bonding hindered the effective packing of nonassociated polymer segments, forming the looser and more disrupted chain packing region. When the HPP content increased to over 40%, as already pointed out in DMTA discussion section, the distribution of hydrogen bonds in the polymer backbone was more random, and the later factor played the main role. The free volume increased with HPP content and reached the highest value at 60 mol % HPP.

Supporting evidence was also from wide-angle X-ray diffraction results. The WAXD diffractograms for homopolymers and two copolymers of PEK-6040 and PEK-4060 are illustrated in Figure 6. It can be seen that all the samples had similar diffraction patterns and displayed amorphous structure due to the presence of bulky pendent cardo groups. However, compared to other three samples, the pattern for PEK-6040 was obviously broadened. Furthermore, relative to PEK-C, the diffraction halos of PEK-4060 shifted toward a smaller diffraction angle (2θ), then the larger angle for PEK-6040, and finally toward the smaller angle again for PEK-H, exhibiting zigzag variation (the dashed line). The interchain *d*-spacing could be calculated from Bragg's equation: $d = \lambda/(2 \sin \theta)$, with θ of maximum of amorphous halo. The *d*-spacings thus obtained are usually taken as the average interchain spacings and used as a measure of the openness of chain packing. Apparently, the variation of *d*-spacings was consistent with the trend of free volume results.

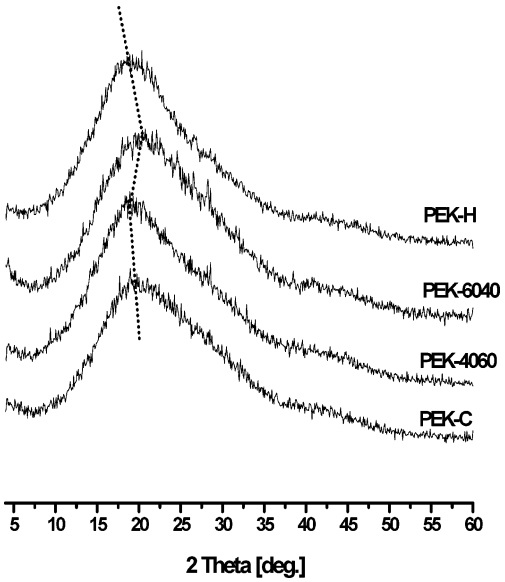

Figure 6. WAXD patterns of the homo- and copolymer membranes.

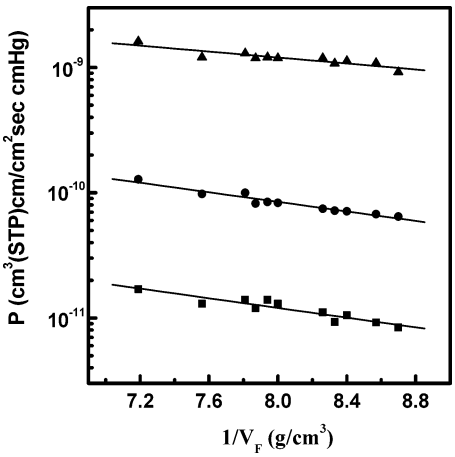

Figure 7. Correlation between permeability coefficients and $1/V_F$ of copolymers.

Scheme 2. Isomerization of Phenolphthalein (PPH) in K_2CO_3 Solution

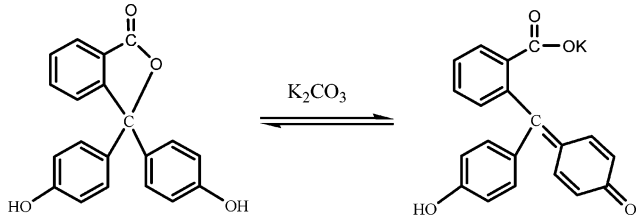

Previous reports had shown that gas permeability coefficients for a given gas in different polymers can be correlated well with the free volume of the polymer according to the following relation:[45−47] $P = Ae^{-B/VF}$, in which the parameters *A* and *B* depend on the type of gas. As illustrated in Figure 7, the gas permeability coefficients for H_2, O_2, and N_2 were linearly correlated well with the inverse of free volume, indicating that chain packing efficiency played a prominent role on the gas

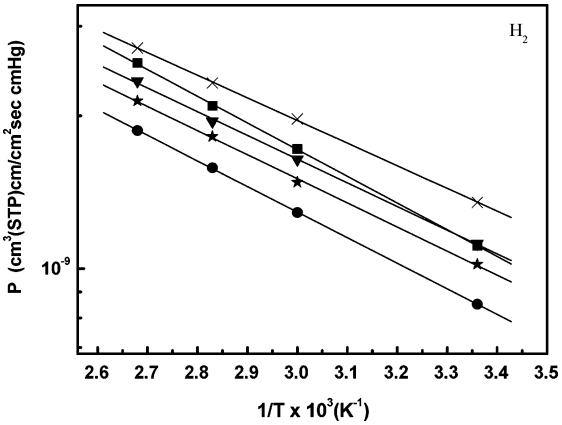

Figure 8. Plots of H_2 permeability coefficients as a function of temperature: (■) PEK-C; (★) PEK-2080; (●) PEK-4060; (×) PEK-6040; (▼) PEK-8020.

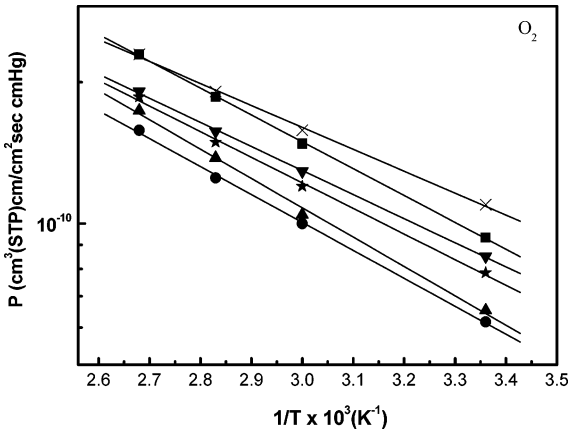

Figure 9. Plots of O_2 permeability coefficients as a function of temperature: (■) PEK-C; (★) PEK-2080; (●) PEK-4060; (×) PEK-6040; (▼) PEK-8020; (▲) PEK-H.

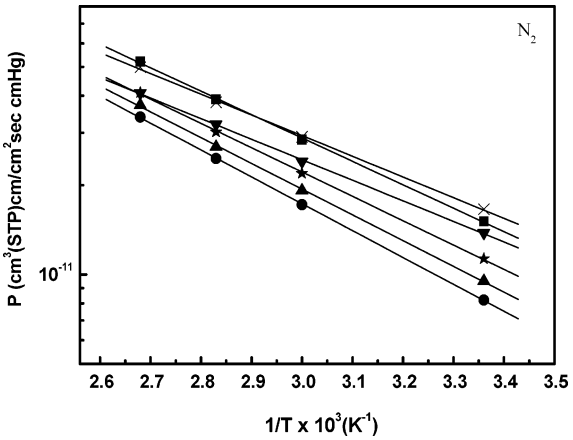

Figure 10. Plots of N_2 permeability coefficients as a function of temperature: (■) PEK-C; (★) PEK-2080; (●) PEK-4060; (×) PEK-6040; (▼) PEK-8020; (▲) PEK-H.

permeation behavior. Consequently, the unusual sigmoid relationship between gas permeability and copolymer composition could be due to the fluctuation in packing density, caused by the interchain hydrogen bonds and change of components in backbone.

Temperature Dependence of the Gas Permeation Behavior. As shown in Figures 8−10, the relationships between gas permeabilities through polymer membranes and absolute temperature were consistent with the Arrhenius equation: $P = P_0 e^{-E_p/RT}$, where P_0 is a preexponential factor, R is the gas constant, and E_p is the apparent activation energy, which can be calculated from the slope of Arrhenius plots. The apparent activation energy data together with the gas permeabilities at 60 and 100 °C are listed in Table 4. Generally, densely packed polymers have less unoccupied "free" space and require larger segmental motions to open a sufficient passageway for permeation. As a consequence, among these three gases, N_2 exhibited the highest permeation activation energy because of its largest

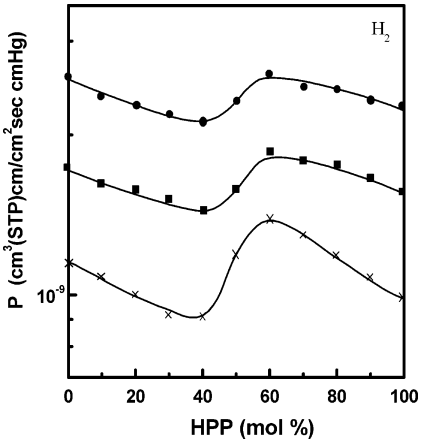

Figure 11. Relationship between H_2 permeability coefficients and HPP content at different temperatures: (×) 30, (■) 60, and (●) 100 °C.

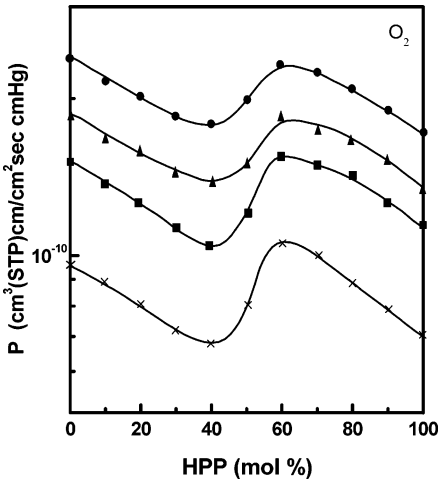

Figure 12. Relationship between O_2 permeability coefficients and HPP content at different temperatures: (×) 30, (■) 60, (▲) 80, and (●) 100 °C.

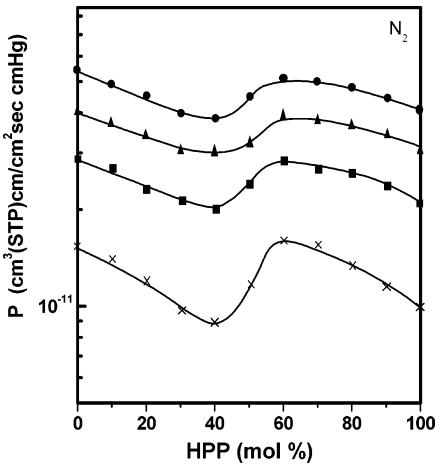

Figure 13. Relationship between N_2 permeability coefficients and HPP content at different temperatures: (×) 30, (■) 60, (▲) 80, and (●) 100 °C.

Table 4. Gas Apparent Activation Energy and Permeability at High-Temperature Data of PEK-C/PEK-H Copolymers

	E_p (kJ/mol)			60 °C				100 °C			
sample	H_2	O_2	N_2	H_2	α_{H_2/N_2}	O_2	α_{O_2/N_2}	H_2	α_{H_2/N_2}	O_2	α_{O_2/N_2}
PEK-C	13.3	14.9	19.3	17.3	60.9	1.51	5.32	25.4	47.3	2.39	4.44
PEK-1090	12.5	13.1	15.0	16.4	63.3	1.38	5.33	24.2	50.1	2.18	4.51
PEK-2080	12.8	14.5	19.3	15.6	66.2	1.27	5.38	22.7	51.7	2.01	4.58
PEK-3070	13.2	14.9	21.9	14.9	69.2	1.16	5.42	21.7	54.2	1.84	4.59
PEK-4060	13.9	15.0	22.8	14.5	71.4	1.12	5.51	21.2	55.2	1.78	4.64
PEK-5050	12.9	14.7	20.9	15.7	67.5	1.20	5.17	23.1	52.2	1.99	4.49
PEK-6040	12.0	12.5	17.8	18.2	64.5	1.55	5.50	25.6	51.3	2.29	4.58
PEK-7030	13.1	13.0	19.0	18.7	66.2	1.48	5.43	25.3	20.9	2.24	4.51
PEK-8020	12.5	13.5	17.8	17.5	66.9	1.40	5.36	24.4	51.2	2.07	4.35
PEK-9010	12.3	13.8	19.8	16.6	69.0	1.27	5.29	23.5	52.9	1.90	4.29
PEK-H	12.2	15.9	21.9	15.7	74.2	1.13	5.36	22.2	54.4	1.71	4.18

molecule kinetic diameter. PEK-4060, which has the smallest free volume, showed the highest permeation apparent activity energy. On the contrary, the loosely packed chain structure led to PEK-6040 the lowest permeation activity energy.

Similar to other glassy polymers, these membranes studied here displayed increased gas permeabilities along with the elevated temperature in the measurement range of 30−100 °C. For PEK-4060 as an example, compared to the gas transport data at room temperature, the permeability coefficients of H_2 and O_2 at 100 °C increased by 147% and 182%, respectively. Moreover, it is noteworthy that, even though the temperature was increased to 100 °C, most of membranes still maintained quite high H_2/N_2 selectivity coefficients, which are even higher than that of bisphenol A polysulfone (PSF) at 30 °C. The simultaneously high gas permeability and selectivity coefficients of this series of polymers are very useful for the high-temperature gas separation application.

Of interest was the observation that, similar to the trend at 30 °C, as shown in Figures 11−13, the gas permeability coefficients at 60, 80, and 100 °C also displayed sigmoid relationships with copolymer composition, but the variation amplitude between wave crest and trough reduced with the increase of temperature. The increasing percentages (I) of gas permeability coefficients for PEK6040 relative to PEK4060 were calculated from eq 4. For H_2, O_2, and N_2 gases, upon increasing temperature, the I values decreased rapidly and then became relatively smooth between 80 and 100 °C (see Figure 14).

$$I(\%) = \frac{P_{\mathrm{PEK6040}} - P_{\mathrm{PEK4060}}}{P_{\mathrm{PEK4060}}} \times 100\% \qquad (4)$$

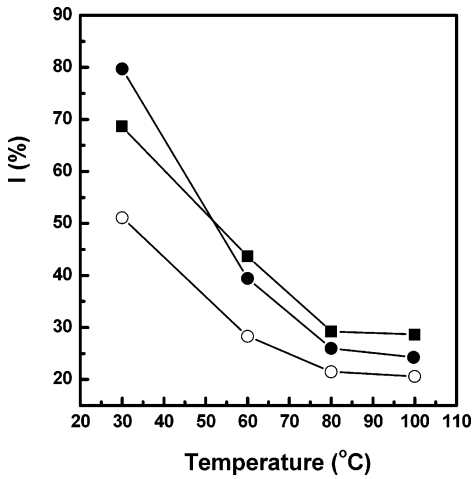

Figure 14. Plots for variation amplitude of permeability coefficients between PEK-6040 and PEK-4060 as a function of temperature: (○) H_2; (■) O_2; (●) N_2.

The DMTA data had shown that all the homo- and copolymers had β and γ transitions at the temperature around 60 and −80 °C, respectively. When the measurement temperature reached 60 °C, the motions of pendent cardo groups and the phenyl rings in the polymer chain around the flexible C−O bond became active, leading to the break of hydrogen bonds and decreased number of the hydrogen bonds with the increase in temperature, which was responsible for the reduction of variation amplitude between wave crest and trough of sigmoid curve at raised temperature. The reason for the smooth reduction trend from 80 to 100 °C is that there was no obvious thermal transition in this temperature range. On the basis of the experimental facts, we can further postulate that, if the temperature could be raised above the glass transition, the interchain hydrogen bonds might completely break, and then the relationship of gas permeability−copolymer composition would have also follow the linear additive rule. The sigmoid dependency of gas permeability on copolymer composition is only a special case for the present hydrogen-bonded copoly(aryl ether ketone) membranes.

Conclusions

The physical and gas transport properties of homo- and copoly(aryl ether ketone) membranes synthesized from phenolphthalein, 3,3′-bis(4-hydroxyphenyl)isobenzopyrrolidone, and equivalent molar bis(4-nitrophenyl) ketone were studied. It was found that the permeability coefficients did not follow the usual property−composition additive rule. In the temperature range of 30−100 °C, the gas permeability coefficients displayed sigmoid relationships with copolymer composition, and the variation amplitude between wave crest and trough was reduced with the increase of temperature. By means of DMTA, X-ray diffraction, density measurement, DSC, and temperature-dependent FTIR methods, the study revealed that this peculiar permeability−composition dependency behavior was attributed to the synergistic effect of two opposing factors caused by the interchain hydrogen bonds, and the hydrogen-bonding effect was reduced with the increase of temperature.

Acknowledgment. The present work was partly supported by the Program for New Century Excellent Talents in University of China (Grant No. NCET-06-0280) and the Scientific Research Foundation for the Returned Overseas Chinese Scholars, State Education Ministry (Grant No. 2005-546).

References and Notes

(1) Camacho-Zuniga, C.; Ruiz-Trevino, F. A.; Zolotukhin, M. G.; Castillo, L. F.; Guzmanb, J.; Chavez, J.; Torres, G.; Gileva, N. G.; Sedova, E. A. *J. Membr. Sci.* **2006**, *283*, 393.
(2) Banerjee, S.; Maier, G.; Dannenberg, C.; Spinger, J. *J. Membr. Sci.* **2004**, *229*, 63.
(3) Xu, Z. K.; Dannenberg, C.; Springer, J.; Banerjee, S.; Maier, G. *Chem. Mater.* **2002**, *14*, 3271.

(4) Handa, Y. P.; Roovers, J.; Moulinie, P. *J. Polym. Sci., Part B: Polym. Phys.* **1997**, *35*, 2355.
(5) Bastarrachea, M. I. L.; Aguilar-Vega, M. *J. Appl. Polym. Sci.* **2007**, *103*, 2207.
(6) Pixton, M. R.; Paul, D. R. *Macromolecules* **1995**, *28*, 8277.
(7) Nagai, K.; Masuda, T.; Nakagawa, T.; Freeman, B. D.; Pinnau, I. *Prog. Polym. Sci.* **2001**, *26*, 721.
(8) Cory, R. J.; Jia, J. P.; Baker, G. L. *Macromolecules* **2000**, *33*, 8184.
(9) Wang, R.; Chan, S. S.; Liu, Y.; Chung, T. S. *J. Membr. Sci.* **2002**, *199*, 191.
(10) Piroux, F.; Espuche, E.; Mercier, R.; Pineri, M.; Gebel, G. *J. Membr. Sci.* **2002**, *209*, 241.
(11) Al-Masri, M.; Fritsch, D.; Kricheldorf, H. R. *Macromolecules* **2000**, *33*, 7127.
(12) Kresse, I.; Usenko, A.; Springer, J. R.; Privalko, V. *J. Polym. Sci., Part B: Polym. Phys.* **1999**, *37*, 2183.
(13) Hamad, F.; Matsuura, T. *J. Membr. Sci.* **2005**, *253*, 183.
(14) Sterescu, D. M.; Stamatialis, D. F.; Mendes, E.; Wu1bbenhorst, M.; Wessling, M. *Macromolecules* **2006**, *39*, 9234.
(15) Alentiev, A.; Drioli, E.; Gokzhaev, M.; Golemme, G.; Ilinich, O.; Lapkin, A.; Volkov, V.; Yampolskii, Y. *J. Membr. Sci.* **1998**, *138*, 99.
(16) Diaz, K.; Vargas, J.; Castillo, L. F.; Tlenkopatchev, M. A.; Aguilar-Vega, M. *Macromol. Chem. Phys.* **2005**, *206*, 2316.
(17) Hu, Y. M.; Sakaguchi, T.; Shiotsuki, M.; Sanda, F.; Masuda, T. *J. Membr. Sci.* **2006**, *285*, 412.
(18) Nagel, C.; Gunther-Schade, K.; Fritsch, D.; Strunskus, T.; Faupel, F. *Macromolecules* **2002**, *35*, 2071.
(19) Wang, Z. G.; Chen, T. L.; Xu, J. P. *J. Appl. Polym. Sci.* **2002**, *83*, 791.
(20) Hiltner, A.; Liu, R. Y. F.; Hu, Y. S.; Baer, E. *J. Polym. Sci., Part B: Polym. Phys.* **2005**, *43*, 1047.
(21) Bondar, V. I.; Freeman, B. D.; Pinnau, I. *J. Polym. Sci., Part B: Polym. Phys.* **2000**, *38*, 2051.
(22) Carrera-Figueiras, C.; Aguilar-Vega, M. *J. Polym. Sci., Part B: Polym. Phys.* **2005**, *43*, 2625.
(23) Kwak, G.; Aoki, T.; Toy, L. G.; Freeman, B. D.; Masuda, T. *Polym. Bull. (Berlin)* **2000**, *45*, 215.
(24) Wang, Z. G.; Chen, T. L.; Xu, J. P. *J. Appl. Polym. Sci.* **1997**, *64*, 1725.
(25) Xu, J. P.; Wang, Z. G.; Chen, T. L. *ACS Symp. Ser.* **1999**, *733*, 269.
(26) Wang, Z. G.; Chen, T. L.; Xu, J. P. *Macromolecules* **2000**, *33*, 5672.
(27) Wang, Z. G.; Chen, T. L.; Xu, J. P. *Macromolecules* **2001**, *34*, 9015.
(28) Baeyer, A. *Ann. Chem.* **1980**, *202*, 80.
(29) Fox, T. G. *Bull. Am. Phys. Soc.* **1956**, *1*, 123.
(30) Sugden, S. *J. Chem. Soc.* **1927**, 1786.
(31) Mikawa, M.; Nagaoka, S.; Kawakami, H. *J. Membr. Sci.* **1999**, *163*, 167.
(32) Ahn, T. K.; Kim, M.; Choe, S. *Macromolecules* **1997**, *30*, 3369.
(33) Lee, L. T.; Woo, E. M.; Hou, S. S.; Forster, S. *Polymer* **2006**, *47*, 8350.
(34) Ting, S. P.; Pearce, E. M.; Kwei, T. K. *J. Polym. Sci., Polym. Lett. Ed.* **1980**, *18*, 201.
(35) Usenko, K. A.; Springer, J.; Privalko, V. J. *J. Polym. Sci., Part B: Polym. Phys.* **1999**, *37*, 2183.
(36) Dorkenoo, K. D.; Pfromm, P. H.; Rezac, M. E. *J. Polym. Sci., Part B: Polym. Phys.* **1998**, *36*, 797.
(37) Shigetoshi, M.; Hiroki, S.; Tsutomu, N. *J. Membr. Sci.* **1998**, *141*, 21.
(38) McHattie, J. S.; Koros, W. J.; Paul, D. R. *J. Polym. Sci., Polym. Phys. Ed.* **1991**, *29*, 731.
(39) Breck, D. W. *Zeolite Molecular Sieves*; John Wiley & Sons: New York, 1994; p 636.
(40) Jeans, J. *An Introduction to the Kinetic Theory of Gases*; Cambridge University Press: London, 1982; p 183.
(41) Hill, A. J.; Weinhold, S.; Stack, G. M.; Tant, M. R. *Eur. Polym. J.* **1996**, *32*, 843.
(42) Burns, R. L.; Koros, W. J. *Macromolecules* **2003**, *36*, 2374.
(43) Goodwin, A. A.; Mercer, F. W.; McKenzie, M. T. *Macromolecules* **1997**, *30*, 2767.
(44) Ghosal, K.; Chern, R. T.; Freeman, B. D.; Daly, W. H.; Negulescu, I. I. *Macromolecules* **1996**, *29*, 4360.
(45) Fujita, H. *Diffusion in Polymers*; Academic Press: New York, 1968; p 75.
(46) Lee, W. M. *Polym. Eng. Sci.* **1980**, *20*, 65.
(47) Maeda, Y.; Paul, D. R. *J. Polym. Sci., Part B: Polym. Phys.* **1987**, *25*, 1005.

MA070426Z